



Subtle structural differences of nucleotide analogs may impact SARS-CoV-2 RNA-dependent RNA polymerase and exoribonuclease activity



Abraham Madariaga-Mazón^{a,b,1,*}, José J. Naveja^{a,e,1}, Arturo Becerra^c, José Alberto Campillo-Balderas^c, Ricardo Hernández-Morales^c, Rodrigo Jácome^c, Antonio Lazcano^{c,d}, Karina Martínez-Mayorga^{a,b,*}

^a Instituto de Química Unidad Mérida, Universidad Nacional Autónoma de México, Carretera Mérida-Tetiz Km. 4.5, Ucú, Yucatán, Mexico

^b Instituto de Investigaciones en Matemáticas Aplicadas y en Sistemas Unidad Mérida, Universidad Nacional Autónoma de México, Sierra Papacál Mérida, Yucatán 97302, Mexico

^c Facultad de Ciencias, Universidad Nacional Autónoma de México, Mexico City, Mexico

^d El Colegio Nacional, Mexico City, Mexico

^e Institute for Molecular Biology and University Cancer Center (UCT) Mainz, Germany

ARTICLE INFO

Article history:

Received 22 March 2022

Received in revised form 5 August 2022

Accepted 27 August 2022

Available online 8 September 2022

Keywords:

SARS-CoV-2

RNA-dependent RNA polymerase

Exoribonuclease

Nucleotide analogs

Molecular modeling

ABSTRACT

The rapid spread and public health impact of the novel SARS-CoV-2 variants that cause COVID-19 continue to produce major global impacts and social distress. Several vaccines were developed in record time to prevent and limit the spread of the infection, thus playing a pivotal role in controlling the pandemic. Although the repurposing of available drugs attempts to provide therapies of immediate access against COVID-19, there is still a need for developing specific treatments for this disease. Remdesivir, molnupiravir and Paxlovid remain the only evidence-supported antiviral drugs to treat COVID-19 patients, and only in severe cases. To contribute on the search of potential Covid-19 therapeutic agents, we targeted the viral RNA-dependent RNA polymerase (RdRp) and the exoribonuclease (ExoN) following two strategies. First, we modeled and analyzed nucleoside analogs sofosbuvir, remdesivir, favipiravir, ribavirin, and molnupiravir at three key binding sites on the RdRp-ExoN complex. Second, we curated and virtually screened a database containing 517 nucleotide analogs in the same binding sites. Finally, we characterized key interactions and pharmacophoric features presumably involved in viral replication halting at multiple sites. Our results highlight structural modifications that might lead to more potent SARS-CoV-2 inhibitors against an expansive range of variants and provide a collection of nucleotide analogs useful for screening campaigns.

© 2022 The Authors. Published by Elsevier B.V. on behalf of Research Network of Computational and Structural Biotechnology. This is an open access article under the CC BY-NC-ND license (<http://creativecommons.org/licenses/by-nc-nd/4.0/>).

1. Introduction

Following the first reports in late 2019, the emergence and rapid spread of the novel coronavirus SARS-CoV-2 has led to a global pandemic infecting more than 530 million persons, killing over six million people, and severely disrupting social and economic order worldwide [1]. Unfortunately, with few exceptions, most countries have been unable to control the spread of the virus, relying on a combination of vaccination campaigns and non-

pharmaceutical interventions such as lockdown and travel restrictions measures.

Despite the unprecedented speed with which various vaccines have been developed, our optimism has been tempered by several issues, including the vaccination rollout, dose shortages, and their glaringly uneven distribution. Even though most of the available vaccines can prevent hospitalizations and deaths, the duration of immunity is still unknown, and not even the best mRNA-based vaccines provide full protection [2]. In addition, although the mutation rate of the SARS-CoV-2 and other coronaviruses ($\sim 10^{-6}$ substitutions per nucleotide per cell infection) is relatively low compared to other RNA viruses [3–6], new variants with high transmission potential and antibody-escape mutations are continuously emerging, e.g. the Delta and Omicron subvariants. The development of vaccines and antivirals with broad-spectrum protection against many human coronaviruses and their variants

* Corresponding authors at: Instituto de Química Unidad Mérida, Universidad Nacional Autónoma de México, Carretera Mérida-Tetiz Km. 4.5, Ucú, Yucatán, Mexico.

E-mail addresses: amadariaga@iquimica.unam.mx (A. Madariaga-Mazón), kmtzm@unam.mx (K. Martínez-Mayorga).

¹ Both authors contributed equally.

could prevent and treat new infections and future pandemics [7,8]. Public health systems are becoming aware that COVID-19 has developed as an endemic and seasonal disease, in addition to the significant number of patients who have developed long-COVID, highlighting the need for pharmacological therapies [9].

1.1. The SARS-CoV-2 RNA-dependent RNA polymerase as a therapeutic target

Coronaviruses are positive-sense, single-stranded RNA (+ssRNA) viruses with a roughly spherical and enveloped architecture of 120–160 nm diameter [10]. They are all part of the family *Coronaviridae*, which consists of five genera, including the *Alpha-*, *Beta-*, *Gamma-*, *Delta-coronavirus*, and the *Alphaletovirus* [11]. Along with the planarian secretory cell nidovirus (PSCNV) (Saberi et al., 2018), coronaviruses are endowed with the largest known RNA viral genomes, ranging from 27 to 32 kb in length [12], and share a similar genome organization, composed of two large open reading frames (ORF1a and ORF1b) plus several structural and accessory proteins nested in the C-terminal end. SARS-CoV-2 has 29 proteins classified as (i) structural proteins, (ii) nonstructural proteins (nsp), and (iii) accessory proteins. Many nonstructural proteins participate in viral replication and transcription, making them attractive therapeutic targets against the SARS-CoV-2.

SARS-CoV-2 replication and transcription processes depend on a multi-subunit complex with structural and functional similarities to the eukaryotic cellular replisome. The RNA-dependent RNA polymerase (RdRp) is a monomeric unit formed by 932 amino acids and is a key component of the SARS-CoV-2 RNA-synthesis molecular machinery. Although there is no evidence of a single origin of RNA viruses, available information shows that all of them have a homologous monomeric RdRp. As of now, the RdRp is the sole recognized universally conserved protein in all RNA viruses and exhibits a remarkable degree of sequence and structural conservation around the active site [13–16]. The RdRp amino acid residues located in the active site participate in metal coordination, binding of the incoming nucleotide, and ribose discrimination [13]. Crystal structures of RdRps of *Coronaviridae* family members [17], including SARS-CoV-2 [18], have confirmed their phylogenetic relationship with those of currently known RNA viruses [13,18,19]. An important difference between the coronaviral and other viral RdRps is the presence of the nidovirus RdRp-associated nucleotidyltransferase domain (NiRAN) in its N-terminus, which is connected to the RdRp by the interface domain [20]. The highly conserved architecture of viral RdRps described above underlines the recognition of this enzyme as a critical target for the design or repurpose of broad-spectrum antiviral drugs in the struggle against the COVID-19 pandemic and future life-threatening viruses.

1.2. The viral proofreading system of exoribonuclease as a therapeutic target

Like other nidoviruses, SARS-CoV-2 encodes a 3'-5' exoribonuclease, whose proofreading activity contributes to the maintenance of its large genome integrity and high genetic stability compared to other RNA viruses [21]. The coronaviral exoribonuclease, also known as nsp14, is composed of two functional domains, the exoribonuclease (ExoN) and a methyl-transferase (N7-MTase), which mediate proofreading during genome replication and support mRNA capping, respectively. Comparisons of the primary and tertiary structures of nidoviral exoribonucleases reveal a high conservation level comparable to that of RdRps. CoV ExoN belongs to the superfamily of exonucleases DnaQ-like endowed with four conserved acidic residues (DEDD) crucial for catalytic activity [22]. Experiments with murine coronavirus lacking ExoN activity have

demonstrated the high susceptibility to the disturbance of the virus replication process, suggesting ExoN as a therapeutic target [23]. However, despite these proofreading capabilities, the eventual appearance of drug-resistant mutants is an inevitable evolutionary process.

A structural model of nsp14-nsp10 suggests a reduced stability of the hydrolyzed form of Remdesivir (monophosphate RDV) in SARS-CoV-2 ExoN. The steric clash between the bulky cyano group on the 1' position of the ribose in RDV with the amide group of the ExoN Asn104 in SARS-CoV-2 models apparently protects RDV from ExoN excision [24]. Furthermore, as opposed to all known cellular exoribonucleases, it has zinc fingers, which opens the possibility of antiviral therapeutic strategies for treating COVID-19 patients [4].

The importance of developing pan-coronavirus antivirals has become clearer with the current pandemic [8]. However, only a few studies have focused on several viral targets as a strategy to stop the proliferation of coronaviruses, such as SARS-CoV-2 [25]. As Rona et al. (2021) demonstrated, the efficacy of remdesivir increases by the combined use of chalcone compounds, such as isobavachalcone or sofalcone. Furthermore, the extraordinary success of drug combinations for treating viral infections provides valuable information for designing treatment guidelines against SARS-CoV-2 [26]. Accordingly, coronaviral exoribonucleases should be considered as a potential target in the designing or repurposing of antiviral drugs, even in combination with RdRp inhibitors [27]. The long-term public health benefits of the use of therapies based on combinations of anti-SARS-CoV-2 inhibitors cannot be ruled out.

1.3. Nucleoside analogs as therapeutic agents

The increased awareness that started in the 1960s of the therapeutic significance of modified nucleosides in the treatment of viral and bacterial infections quickly led to the syntheses of small molecules that do not destroy viral pathogens but rather inhibit their replication and transcription [28,29]. The study of nucleoside analogs as antiviral agents has undergone extraordinary advancements, from the original empirical viral infection inhibition with purine analogs painstakingly synthesized in the laboratory [30], to *in silico* methodologies that allow the rapid identification of nucleoside analogs with potential antiviral activity by inhibiting viral replication or transcription [31].

The cryo-EM and molecular modeling studies have led to a substantial understanding of the mechanism of inhibition of RdRp at atomic resolution. Moreover, nucleotide analogs have been proposed as RdRp modulators, based on protein tertiary structure comparisons, molecular modeling studies, virtual screening campaigns, *in vitro* assays, and clinical trials [26,32–35]. The cryo-EM structures reported by Yin et al., which include the monophosphate form of Favipiravir, Ribavirin, and penciclovir covalently linked to the primer strand, show that they act as immediate chain terminators [36]. Similarly, other nucleotides, such as RDV and β -D-N4-hydroxycytidine, bind in the pre-catalytic state [37]. The post-translocation stage has been observed only for the natural nucleoside triphosphate NTPs [36]. The cryo-EM structure of Remdesivir monophosphate (RDV-MP) bound to the SARS-CoV-2 RdRp shows that it blocks RNA translocation after incorporating three bases following RDV-MP, resulting in delayed chain termination [38]. Additional studies showed that mutations of nsp12 (Ser861) reduce the inhibitory effect of RDV [39,40]. The structure also revealed that the cyano group, which is located at the 1' carbon of the ribose of each RDV-MP molecule, is readily accommodated in the active site, without apparent steric interactions. Thus, a steric interaction is expected to occur as the RNA duplex attempts to translocate to allow the binding and incorporation of UTP. Nevertheless, the inhibition mechanism of RDV is not simple.

Studies with MERS-CoV have shown that the arrest of RNA synthesis occurs three nucleotides after RDV is incorporated into the nascent RNA [40]. This suggests that the nsp14 exonuclease proofreading domain might detect a base pair mismatch and activate its exonuclease activity, thus resulting in the stalling of the polymerase complex [39].

RNA viruses are well-known for their high mutation rates [32]. However, this is a broad generalization, as coronaviruses display a lower mutation rate than expected since they are the only known RNA viruses that encode a proofreading exonuclease (nsp14) [3,4,41]. Nsp14 is also present in SARS-CoV, where it has been found to exert its exonuclease activity associated with nsp10 [26]; the nsp14 protein has a second domain with methyltransferase activity for mRNA capping [33,42]. The presence of a large complex of nsp7-nsp8-nsp12-nsp14 suggests that the polymerization and the proofreading activities occur simultaneously [34].

A large clinical trial demonstrated that following the infection, by day 29, RDV reduced mortality in hospitalized COVID-19 patients from 15.2 % to 11.4 % [43] and has reached clinical approval by public agencies in the treatment of severe COVID-19 [44]. Nucleotide analogs appear to inhibit the replication of SARS-CoV-2 in early clinical trials [26,41,43,45–47]. The list includes Sofosbuvir (SOF), Favipiravir (FPV), Molnupiravir (MPV), Ribavirin (RBV), and RDV which are ribonucleic analogs that, in principle, could act as inhibitors of RdRp and stop viral RNA synthesis. While RDV is a new generation drug that failed to prove efficacy against the Ebola virus in clinical trials [48], SOF is an FDA-approved drug recognized as an effective treatment against chronic infection by the hepatitis C virus [49].

Based on *in silico* and *in vitro* assays, many molecules, mainly nucleoside analogs, have been proposed as antivirals to fight COVID-19, but only a handful of them have been approved as therapeutic options against the SARS-CoV-2. Remdesivir (RDV) is an adenosine analog that is incorporated into the growing viral RNA chain resulting in the stalling of the RNA-dependent RNA polymerase (RdRp) [50,51]. The efficacy of this drug is still controversial due to the uncertain effectiveness of hospitalized patient recovery, the null reduction of mortality, and its high cost. However, the FDA approved RDV as an emergency drug use, while the CDC recommended its use in hospitalized adult patients with COVID-19 that require minimal supplemental oxygen (<https://www.covid19treatmentguidelines.nih.gov/management/clinical-management/hospitalized-adults-therapeutic-management/>), and the WHO included a conditional recommendation against the use of this antiviral. More recently, the FDA and the MHRA approved molnupiravir (MNV) to treat adult patients with mild-moderate COVID-19 who are at risk of severe forms of the disease. MNV is a cytidine analog that also affects the RdRp activity, albeit by a different mechanism, i.e. lethal mutagenesis [52]. MNV triphosphate, the active form of the drug, is incorporated into the growing RNA chain in the place of cytidine. However, in its imino form, MNV serves as a template for adenosine, which leads to the binding of uracil in the next round of replication, resulting in an increase of C to U mutations [50,53]. Preliminary results (Merck's report – October 1, 2021) of MNV's clinical trials were encouraging, yielding a 50 % reduction in the rate of hospitalization and/or death from COVID-19 [54]. However, the results of the trial reported a more discrete 30 % reduction (Merck's report - November 26, 2021) [55]. Sofosbuvir (SOF), another nucleoside analog, has a proven safety profile, is used to treat chronic hepatitis C, and has been proposed as a potential alternative to treat the SARS-CoV-2 infection [56]. SOF is a uridine analog that binds to the RdRp active site and blocks the conformational changes of S282, preventing the incorporation of incoming nucleotides [57], arresting RNA synthesis.

In this work, we report the potential binding of a comprehensive build-to-purpose nucleotide analog database at three key

positions of the replication process of SARS-CoV-2 and report the outcomes building upon previous studies on RDV, SOF, FPV, MPV, and RBV.

2. Results

The five reference RdRp nucleotide inhibitors (RDV, SOF, FPV, MPV, and RBV) were docked and analyzed in three key positions on the RdRp-ExoN complex (RdRp-catalytic site, RdRp-cat; nucleotide in position $i + 4$ of nascent RNA in RdRp, RdRp-p4; and catalytic site of exonuclease, ExoN-cat). Graphical representations of the binding pose at each position are depicted in Fig. 1. Then, a database of 3D nucleotide analogs assembled from PubChem was docked at each position. Based on a combined score, we identified seven computational hits that are predicted to fit into the three explored key locations and with the potential to block replication by steric hindrance with relevant residues. In addition, we analyzed the effect of the substituents in the predicted binding positions; our results provide useful hits and may assist in the design of new nucleotide analogs.

2.1. Docking into the RdRp catalytic site

To explore the mode of interaction of the reference drugs (SOF, RDV, FPV, MLV, and RBV) in the catalytic site of the RdRp, two docking simulations were performed with distinct RdRp crystallographic structures (see Fig. S1). The first one corresponds to the complex with FPV in its triphosphate form (PDB ID: 7CTT), and the second one is a complex with RDV in its monophosphate form, bound to the template-primer RNA (PDB ID: 7BV2). Table 1 shows the docking scores obtained for the reference drugs in three relevant binding sites of the protein complex. In all cases, nucleotides were used in monophosphate form.

As expected, RDV has the highest docking score among the five drugs. Interestingly, RDV is the only molecule that interacts with Lys545 through a hydrogen bond interaction (2.4 Å). Lys545 is involved in the nucleotide triphosphate entry (NTP) of the RdRp. In all cases, side-chain acceptor interactions with Arg555 are present. For all triphosphate forms of the drugs, the interaction of the phosphate groups with Arg553, Asp618, Asp760, and Lys798 are observed, suggesting that the conformation adopted in the catalytic site is favorable for hydrolysis of the pyrophosphate group, preceding a conformational change to coordinate the divalent cations [58]. In addition, in the five drugs analyzed, hydrogen bonds are formed between the complementary base in the template RNA chain and the drug heterocyclic base. The results obtained from the docking studies with the RdRp co-crystallized with RDV-MP suggest that, with the sole exemption of MPV, all drugs are predicted to bind in a similar manner.

2.2. Nucleotide analogs database

A total of 517 compounds were virtually screened in the systems described above: RdRp-cat, RdRp-p4, and ExoN-cat. Of them, 167 have one ring and 350 have two or more rings in the nitrogenous base, thus corresponding to pyrimidine or purine analogs, respectively. Interestingly, purines seemed to have overall better scores in the three systems (see Fig. 2). Not surprisingly, the scores of purine analogs were not as good when the complementary base was also a purine. In addition to the canonical substitutions, we explored the performance of nucleotides with substitutions in the ribose scaffold, (see Fig. 2). Overall, the nucleotides substituted at C1' have a better fit in the three studied systems. Moreover, the cyano substitution improved the consensus binding score. Substitutions at the C2' position did not improve docking scores in gen-

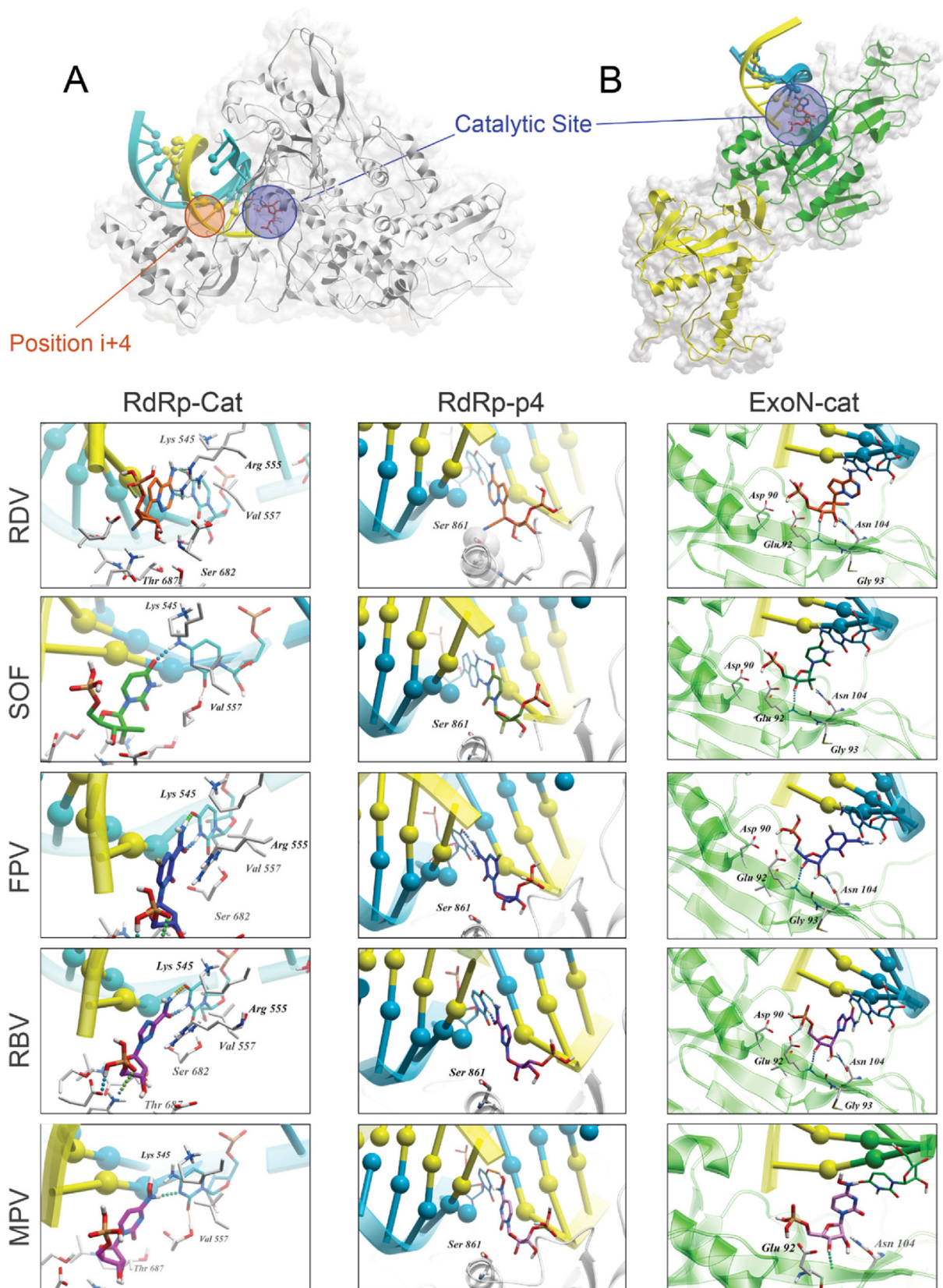


Fig. 1. Relevant positions for binding in the RdRp – exonuclease system. The catalytic and $i + 1$ positions are shown in panel A a 90 rotation in the z-axis is shown in panel B. Images underneath show each of the binding poses obtained for the reference nucleotides at the three relevant positions of the protein complex.

eral but had a more positive effect when the complementary nitrogenous base was a purine. In the molecules studied, substitutions at the C3' position do not seem to impact docking scores at

RdRp-cat, while leading towards worse scores at RdRp-cat, but only 12 were substituted in this position. Molecules with C4' non-canonical substitutions have better docking scores when the

Table 1

Docking scores calculated for the five drugs at three relevant binding sites of the protein complex.

	RdRp-cat	RdRp-p4	ExoN-cat
FPV	-19.07	-19.27	-16.18
MOL	-17.98	-17.37	-16.80
RDV	-26.74	-23.29	-17.94
RBV	-16.66	-20.47	-22.80
SOF	-19.22	-17.25	-17.30

complementary base is a purine, but they showed no overall difference at the different docking sites. Lastly, substitutions at the C5' position led to worse scores in the studied systems, also with positive effects when the complementary base was a purine. Considering that a clash at the RdRp-p4 is desirable for disrupting the

enzyme's activity, C3' substitutions might be worth exploring in further studies, as they seem to still fit well at RdRp-cat. Noteworthy, this analysis predicts unfavorable scores for C2', C4', or C5' substitutions.

2.3. Consensus scoring

Given the non-linearity of docking scores (RMSEA: 0.085; CFI: 0.53), the model for consensus scoring had an acceptable fit. Tables 2 and 3 show the point estimates for the loadings of latent variables and their covariance matrix, respectively. Of note, the covariances between site scores are all positive, implying that molecules having better scores in one site are expected to have better scores in the others as well.

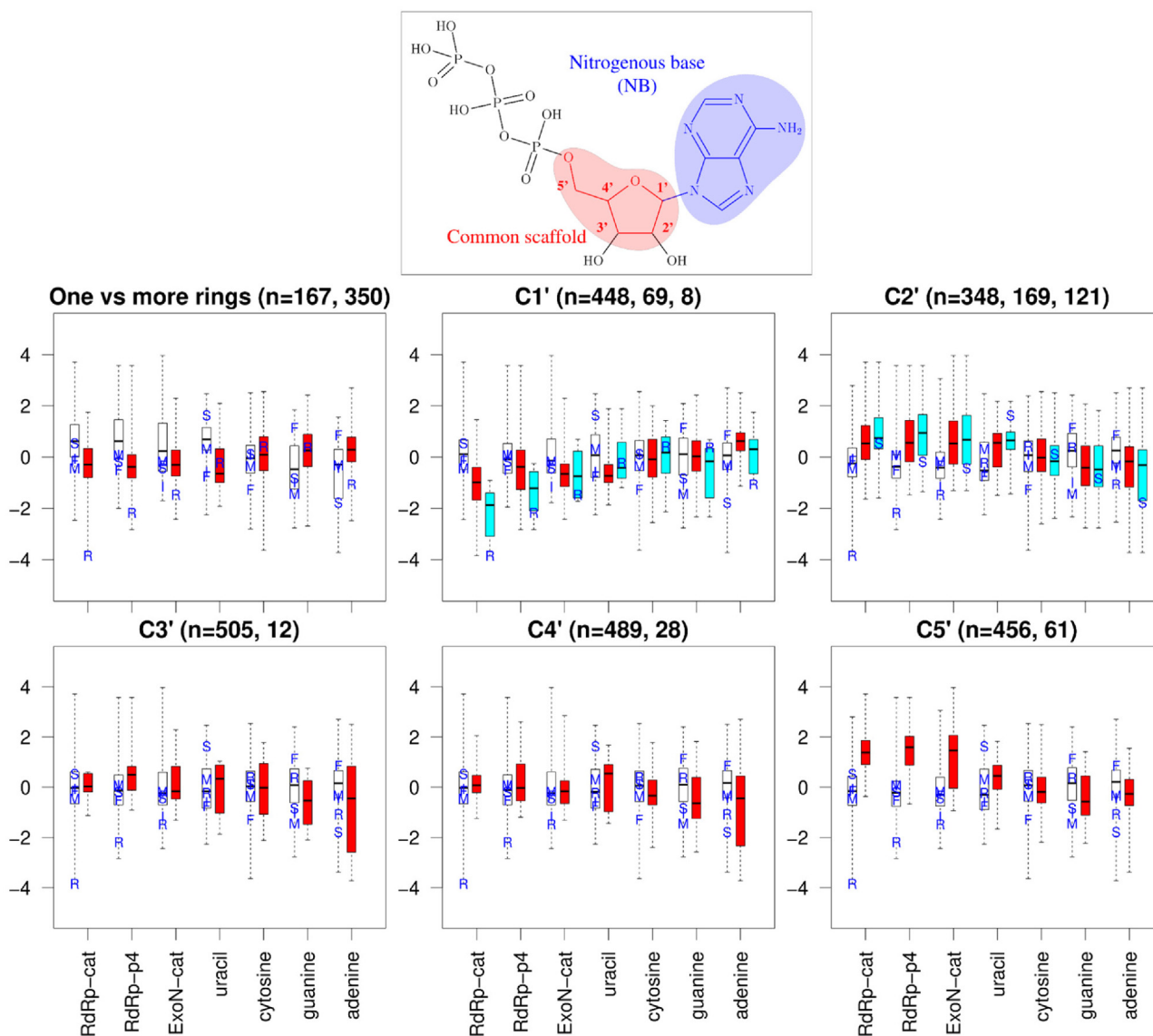


Fig. 2. Substituent analysis. The chemical structure of ATP is shown above, highlighting in red the common scaffold for the molecules in the database and the substitution sites, and with the nitrogenous base shown in blue (note that adenine is a purine, i.e., it has two connected rings). The box plots depict the distribution in the different consensus scores. Consensus scores include the three docked sites (RdRp-cat, RdRp-p4 and ExoN-cat), and the score when using a certain complimentary base (uracil, cytosine, guanine, or adenine). Different subgroups are compared in the boxplots: compounds with one vs more rings in the nitrogenous base (i.e., similar to pyrimidine or purine, respectively), and substitutions in the ribose carbons other than the canonical (being the canonical form the one shown for ATP above). To ensure a better graphical representation, all variables were standardized by subtracting the mean and dividing by the standard deviation. For all variables, a lower value implies a better fit. In white, molecules with the canonical substitution; in red, molecules with other substitutions; in cyan, molecules with a cyano group in C1' or a fluorine in C2'. The scores of reference compounds are presented in blue letters as a reference (R: Remdesivir, S: Sofosbuvir, F: Favipiravir, M: Molnupiravir, I: Ribavirin). In all box plots, the box limits represent the first and third quartile, whereas the thick middle line depicts the median. The whiskers extend up to the minimum and maximum observed values. The subgroup size is presented above the corresponding panel. (For interpretation of the references to colour in this figure legend, the reader is referred to the web version of this article.)

Table 2
Latent variables loadings estimated for the model in Fig. 1. *: $p < 0.05$. NB: nitrogenous base.

	Load	RdRp-cat				RdRp-p4				ExoN-cat			
		A	C	U	G	A	C	U	G	A	C	U	G
APF	site	1.00	1.16*	1.13*	1.4*	1.00	91.10	77.5	74.47	1.00	2.75*	1.49*	0.56*
	NB	1.00	1.00	1.00	1.00	98.52	-0.09*	0.21*	0.05	-50.19	-0.10*	0.01	0.07*
DockingScore	site	0.13*	0.11*	0.26*	0.12*	2.38	60.05	68.24	62.94	0.68*	1.47*	0.64*	0.40*
	NB	42.43	4.73	0.39*	0.25*	120.18	0.03	0.50*	0.18*	39.66	0.01	-0.01	0.13*
HB	site	0.02*	0.02	0.05*	0.03*	-2.63	0.691	9.68	4.69	0.12*	0.16*	0.07*	0.14*
	NB	3.82	0.04*	0.12*	0.09*	13.58	~0.00	0.13*	0.03*	2.42	-0.01	0.02*	-0.01*
S861	site	-	-	-	-	1.50	-1.21	2.5	3.69	-	-	-	-
	NB	-	-	-	-	2.01	0.01	0.01*	~0.00	-	-	-	-
N104	site	-	-	-	-	-	-	-	-	0.04*	0.08*	0.06*	0.02*
	NB	-	-	-	-	-	-	-	-	-1.03	~0.00	0.01	~0.00

Table 3
Covariance matrix between latent variables. *: $p < 0.05$.

	cat	i + 4	ExoN	U	C	G	A
cat	69.62	0.297	10.187*	-	-	-	-
i + 4	0.297	0.003	0.079	-	-	-	-
ExoN	10.187*	0.079	5.394	-	-	-	-
U	-	-	-	74.014	-3.071	-1.852	-0.102
C	-	-	-	-3.071	12.328	1.949	0.009
G	-	-	-	-1.852	1.949	141.934	0.107
A	-	-	-	-0.102	0.009	0.107	0.001

2.4. Best computational hits

The selection of the most promising hits relied on the assumption that any effective compound must be incorporated into the nascent RNA strand. Therefore, we selected only molecules with a consensus RdRp-cat (7CTT) latent score below two standard deviations from the mean, and both RdRp-p4 and ExoN-cat consensus scores below one standard deviation. Seven molecules (Table 4) passed these consensus filters. Hence, we propose the seven molecules shown in Table 4 as promising candidates against SARS-CoV-2 RdRp. Fig. 3 shows the distribution of the molecules in the consensus scores for the three studied systems and Fig. 4 shows their chemical structures and details of their interaction with the RdRp-ExoN systems.

3. Discussion

We report an integrative approach for exploring the structural features relevant for designing nucleotide SARS-CoV-2 RdRp inhibitors. Docking poses of the co-crystallized ligands RDV-MP and FPV-MP reproduced the corresponding experimental conformations with RMSD values below 1.0 Å. Then, we modeled a database of nucleotide analogs as an exploratory tool to determine their potential inhibitory activity. Under the conditions studied here, RDV exhibited the best docking scores among the 517 nucleotide analogs analyzed in RdRp-cat. Our results highlight RDV as a potentially dual RdRp and ExoN inhibitor against SARS-CoV-2 [59]. As detailed below, we identified a number of molecules with high predicted affinities towards RdRp-p4 and ExoN-cat, thus representing potential candidates for developing new antivirals. The extent to which the ExoN inhibition would be beneficial in combating the SARS-CoV-2 infection remains to be explored [4,42].

These last two years have shown that the SARS-CoV-2 and COVID-19 are far trickier than originally thought. Clearly, the major significant shift was the development of numerous safe and effective vaccines and the massive vaccination campaigns implemented throughout the world. However, different factors have demonstrated that vaccination by itself is not going to be the coveted panacea, and that research efforts aimed at better

understanding the disease and finding alternatives to treat it are far from over.

Long COVID, also known as Post COVID-19 condition, defined as the persistence of symptoms 12 weeks after the first acute SARS-CoV-2 infection, affects millions of individuals worldwide [60] and over 50 different symptoms have been associated with this condition [61]. The ultimate cause of this pathology remains an open issue, and different ideas have been posited as its main contributors, including the formation and deposition of blood clots, alterations in the immune system, the persistence of replicating virus in various tissues including the intestinal epithelium, or a combination of all of them [62–65]. A related, but slightly different scenario, is represented by immunocompromised patients, in which the virus continues its replication for months [66,67]. One of the consequences of the prolonged viral replication is the inevitable intra-host SARS-CoV-2 evolution. The regular viral sequencing of these patients revealed, perhaps not surprisingly, the presence of several of the immune-escape mutations which would later characterize the variants of interest and of concern, a phenomenon that may have been associated with the emergence of some of the circulating variants of concern [68].

Major efforts to find effective drugs against SARS-CoV-2 were undertaken by the scientific community around the globe during the first months of the pandemic [69]. The current COVID-19 therapeutic panorama is encouraging, with drugs approved for each phase of the disease, including antivirals, Janus kinase inhibitors, IL-6 receptor blockers, corticosteroids, monoclonal antibodies [70]. Nonetheless, the elevated vaccination rates and the predominance of VOCs like Omicron and its subvariants, which are characterized by relatively milder clinical manifestations, have been diminishing the interest in the search for antivirals [71]. Moreover, from a strategic perspective, the extremely high number of previously infected persons and the existence of approved antivirals against the COVID-19, e.g. molnupiravir and nirmatrelvir/ritonavir, have complicated the recruitment of “naive” individuals which might be included in proposed antivirals clinical trials. And yet, the quest for a wider array of anti-COVID drugs should be warranted by several factors, including the inevitable evolution of the SARS-CoV-2, which has led to new infection waves caused by recently-emerged variants with higher transmissibility and better-

Table 4

References and most promising compounds (hits) against SARS-CoV-2 RdRp and ExoN in the nucleotides database. Only latent variables related to the docking site consensus are shown.

Molecule name or PubChem CID	DB ¹	Consensus RdRp-cat	Consensus RdRp-p4	Consensus ExoN-cat
FPV	REF	-0.15	-0.51	-0.33
MPV	REF	-0.44	0.07	-0.18
RBV	REF	-0.06	0.09	-1.16
SBV	REF	0.53	-0.19	-0.43
RDV	REF	-3.85	-2.18	-1.47
24,763,257	RDV	-2.46	-1.28	-1.26
25,245,386	FPV, MPV, RBV	-2.14	-1.40	-1.68
440,059	MPV	-2.44	-1.23	-1.45
46,874,980	RDV	-2.22	-1.19	-1.06
68,658,112	RDV	-2.44	-2.64	-1.69
70,587,122	RDV	-3.72	-2.84	-1.72
70,907,629	RDV	-2.46	-2.00	-1.70

¹ DB: Source database of molecules. REF: reference drugs; RDV: analog to Remdesivir; FPV: analog to Favipiravir; MPV: analog to Molnupiravir; RBV: analog to Ribavirin.

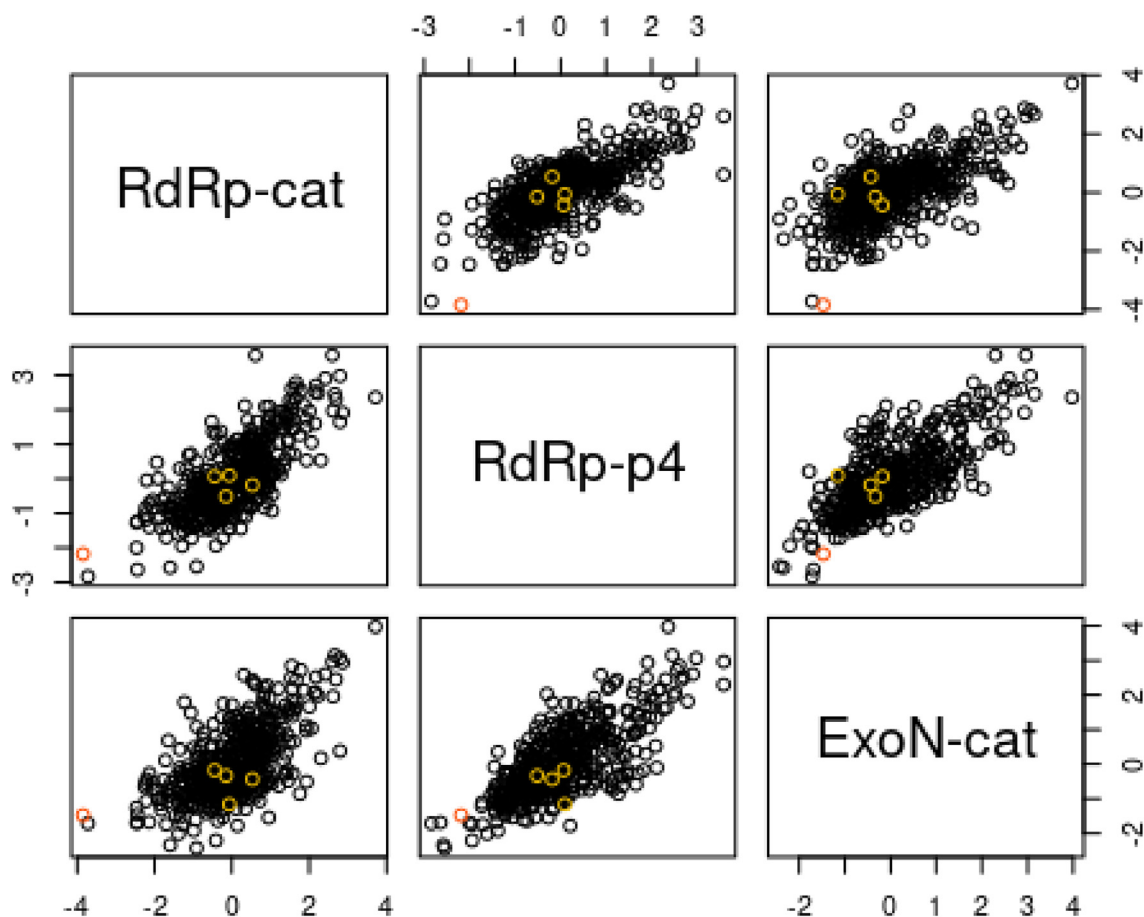


Fig. 3. Pairwise plots of the consensus scores at the three docking sites. RDV-MP is marked in red, and the other references in orange. Note that RDV-MP has excellent performance in all docking sites. (For interpretation of the references to colour in this figure legend, the reader is referred to the web version of this article.)

tuned immune escape capabilities; the fact that immunocompromised patients may benefit from shorter infections hindering the possibility of incubating potential new variants; and the growing evidence that Long COVID might be partly due to a persistently replicating virus. Hence, the importance of *in silico* and *in vitro* studies such as those reported here that allow us to test new treatments and model their plausible molecular interactions.

The strong selective pressures from the immune system and the introduction of vaccines have driven the spike protein to display a faster evolution. However, the nsps encoded by ORF1a/b have had two mutations so far, at least in the RNA-dependent RNA

polymerase, and the key role that these proteins play in viral replication and maturation reduces the possibility that drug-resistant variants will emerge as fast as mAb-escape variants did [72]. Therefore, a combinational approach of nucleoside analogues, including favipiravir, ribavirin, and remdesivir (but also sofosbuvir and molnupiravir as shown in this study) may have a synergistic effect to inhibit the viral replication as seen in other RNA viruses [73]. Moreover, a therapy based on rational combinations of anti-SARS-CoV-2 inhibitors against different viral components such as the RdRp, the exonuclease or the proteases, might help enhance the treatment's potency, mitigate side effects as much

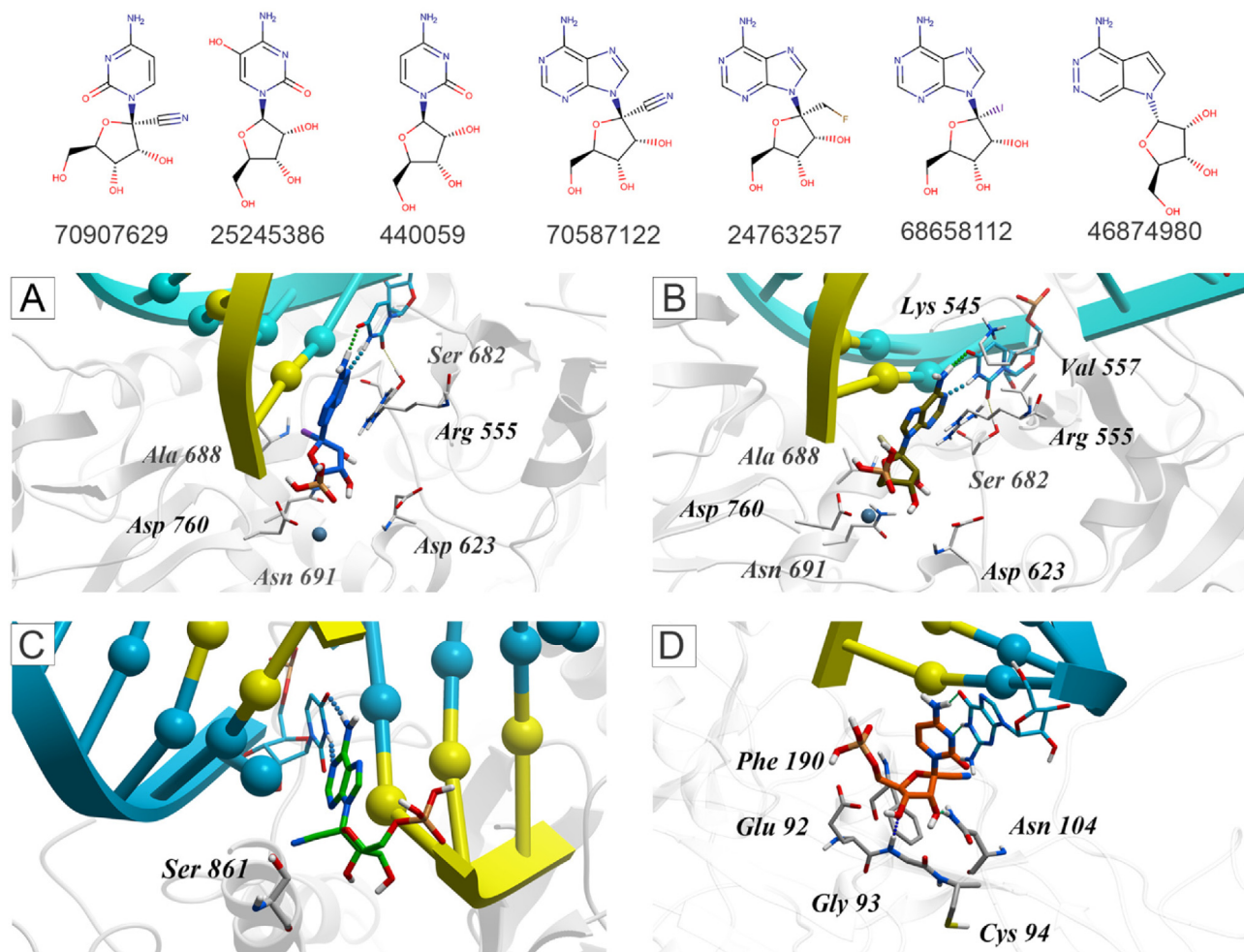


Fig. 4. Binding modes of selected nucleotide analogs. Upper panel: the top seven selected molecules, identified by its PubChem CID. Lower panel: details of binding mode for (A) analogue 68,658,112 (cyan sticks) and (B) analogue 24,763,257 (olive sticks) into RdRp-Cat system (grey cartoon and white sticks); (C) analogue 70,587,122 (green sticks) into RdRp-p4 system (grey cartoon and grey sticks); and (D) analogue 70,907,629 (orange sticks) into the ExoN-Cat system (grey cartoon and grey sticks). (For interpretation of the references to colour in this figure legend, the reader is referred to the web version of this article.)

as possible, and avoid drug-resistant mutants [74]. Notably, the effect of nucleotides at the exonuclease proofreading site has not been extensively explored or used as a strategy for RdRp regulation [28,39]. Based on this area of opportunity, we show in this work that the simultaneous targeting of multiple sites in the replication process seems feasible and worth pursuing. To evaluate this hypothesis, we are performing *in vitro* evaluations of nucleotide analogues, the results will be publicly available in due course.

4. Conclusion

In summary, we presented the structural analysis of five relevant nucleotide drugs against the RdRp and ExoN of SARS-CoV-2. To extend the study to other similar molecules, a database of 517 analogs of these drugs was curated. Through the analysis of this database, we anticipated that, besides the classical C1' substitution exemplified by RDV, C3' substitutions might be of interest in the development of SARS-CoV-2 RdRp inhibitors. The resulting collection of molecules could be a starting point for other projects aiming at studying nucleotide analogs through molecular modeling, as we considered phosphorylation status and stereochemistry in the assembly of the data.

Approaches that target or modulate essential and well-conserved nonstructural proteins such as the RdRp and the exonuclease can be capable of a pan-coronavirus antiviral activity against emergence and re-emergence of highly pathogenic diseases.

5. Materials and methods

5.1. Nucleotides database: compilation, curation, and R-group decomposition

A molecular database of nucleotide analogs was built by searching the PubChem (<https://pubchem.ncbi.nlm.nih.gov/>) database using as a template the three-dimensional structures of RDV, SOF, RBV, FPV, and MPV. The SMILES (Simplified Molecular Input Line Entry System) codes of drugs and analogs were retrieved and saved in SDF format. The nucleotide database was organized as an R-group table. The remaining compounds were automatically phosphorylated using SMIRKS in RDKit, version 2020.09.1 (<https://www.rdkit.org/>). Mono- and tri-phosphorylated forms of all except five nucleotides, which lack an accessible hydroxyl group, were obtained. After eliminating duplicates from the database, 517 phosphorylated nucleotides remained and were used for molecular modeling studies (Supplementary Table S1).

5.2. Docking simulations

Docking simulations of RDV, SOF, FPV, MPV, RBV, and their analogs from the curated database were performed using the software ICM (Internal Coordinate System, Molsoft Inc.) 3.9-2b [75]. The tertiary structures of RdRp in complex with FPV (PDB ID: 7CTT) and RDV in the catalytic site (PDB ID: 7BV2) were retrieved from the PDB database. These systems include the NSP12-NSP7-NSP8 complexes, as well as a translocated RNA molecule. Docking in exoribonuclease was prepared following the same protocol but using a homology-modeled protein built as described below. The proteins were prepared in ICM, setting the protonation at pH = 7.0, checking for protomers, assigning tautomers, and performing a geometry minimization. The docking was performed by a two-step protocol: a placement process by a flexible alignment; and a docking scoring refinement calculation. The docking score was obtained directly from ICM software, which is a GBSA/MM-type scoring function augmented with a directional hydrogen bonding term [76]. The predicted pose was compared to the conformation of the natural nucleotide and measured by the atomic property field (APF) approach [77]. Using this methodology, seven molecular properties are calculated: (hydrogen bond donors and acceptors, sp² hybridization, lipophilicity, size, charge and electropositivity or electronegativity). That information is used for the superposition of ligands on one or multiple molecular templates by Monte-Carlo minimization in the atomic property fields potentials combined with standard forcefield energy. As a result, an APF value (APF score) is obtained and related to 3D-conformational similarity with a molecule reference. In addition, a score that takes into account the hydrogen bonds that are formed between the ligand and the residues of the protein in the binding site was calculated. This score, denoted as “HB”, was calculated for those hydrogen bonds between the nucleotide of the complementary base and the docked nucleotide analog. In both cases, the lower the score value, the better conformation (APF) or better HB formation (HB). Finally, from the docked poses, we measure the distances of each docked nucleotide (center of mass) to the residues involved in known steric clashes related to potential inhibition of the RdRp activity. These residues are serine 861 (S861) in the system RdRp-p4, and asparagine 104 (N104) in the ExoN-cat system.

5.3. RdRp mutants with the different nitrogenous base combinations

In order to set the correct nitrogenous base pair between the docked molecule and the RNA template, the corresponding nucleotide mutations were performed in each of the three systems studied (RdRp-cat, RdRp-p4, ExoN-cat). For this endeavor and following the canonical Watson-Crick pairing adenine-uracil and guanine-cytosine, a total of twelve systems were built. The resulting models were prepared for docking simulations as previously described.

5.4. Flexible alignment

Nucleoside drugs (RDV, SOF, FPV, MPV, and RBV) were placed into the binding site of RdRp, using a flexible alignment protocol available in MOE, taking as reference the co-crystallized ligand,

FPV, in the catalytic binding site (PDB ID: 7CTT). The calculation was terminated when at least 50 conformers were collected throughout 200 iterations. The conformations were chosen by random rotations in the rotatable bonds, with a limit of 100 configurations. The orientation was found by minimizing the similarity function, where F is the similarity feature of the property densities between pairs of atoms, and U is the average potential energy with the force field MMFF94x.

5.5. Homology modeling of SARS-CoV-2 exoribonuclease

We built a homology model of SARS-CoV-2 NSP14 using the publicly accessible Swissmodel suite [78]. The crystallographic structure of SARS-CoV NSP14 guanine-n7 methyltransferase (PDB ID: 5C8S) was taken as a template, according to the alignment search (basic local alignment search tool, BLAST) performed with the SARS-CoV-2 NSP14 sequence obtained from Uniprot database (accession code: P0DTD1; “Replicase polyprotein 1ab”). The resulting modeled protein was analyzed using MolProbity for clashes [79]; Ramachandran favored torsion angles; rotamer outliers; and bad angles and bonds. Next, a superposition of modeled SARS-CoV-2 NSP14 and the crystallized SARS-CoV NSP14 (PDB ID: 5NFY) was performed in order to assess the correct tertiary structure of the model. The RNA and the magnesium and zinc ions were added to the SARS-CoV-2 ExoN model using as a template the crystallographic structures of Lassa nucleoprotein with triphosphate RNA (PDB ID: 4FVU and PDB ID: 4GV9). Finally, the model was energy-minimized using the Amber10:EHT forcefield with charges from the force field and a gradient cutoff of 0.01 RMS kcal/mol/Å². The resultant model was analyzed using MolProbity. By the time of this work, the X-ray structure of the ExoN became available. The RMSD value between the X-ray structure and our homology model is 0.23 Å, indicating nearly identical structures.

5.6. Consensus scoring through structural equation modeling

The variables investigated through docking simulations are: APF, docking score, hydrogen bond interactions, predicted energy, and the distance to selected residues (only in i + 4 and ExoN). As mentioned above, docking systems were built by mutating pair bases in the template RNA sequence; in total, 44 variables were obtained (Table 5).

To generate consensus scores that considered all the variables while reducing the dimensionality of the data, we constructed a structural equations model through lavaan R's package with the factorial design [80] presented in Fig. 5. This model estimates latent (not directly observable) site consensus variables that can be indirectly measured through the variables observed in docking. In the model, we also include latent variables to account for the effect of mutations in the template chain. As depicted in Fig. 5, the model estimates correlations among the latent variables for mutations and site consensus separately, but not between mutations and site consensus. Root mean square error approximation (RMSEA) and comparative fit index (CFI) were measured as goodness-of-fit statistics.

Table 5
Variables considered for the consensus model.

Site	Variables	Systems with different pair bases in the template RNA	Number of variables
RdRp-cat	APF, Docking score, HB	4	12
RdRp-p4	APF, Docking score, HB, S861	4	16
ExoN-cat	APF, Docking score, HB, N104	4	16
Total	–	–	44

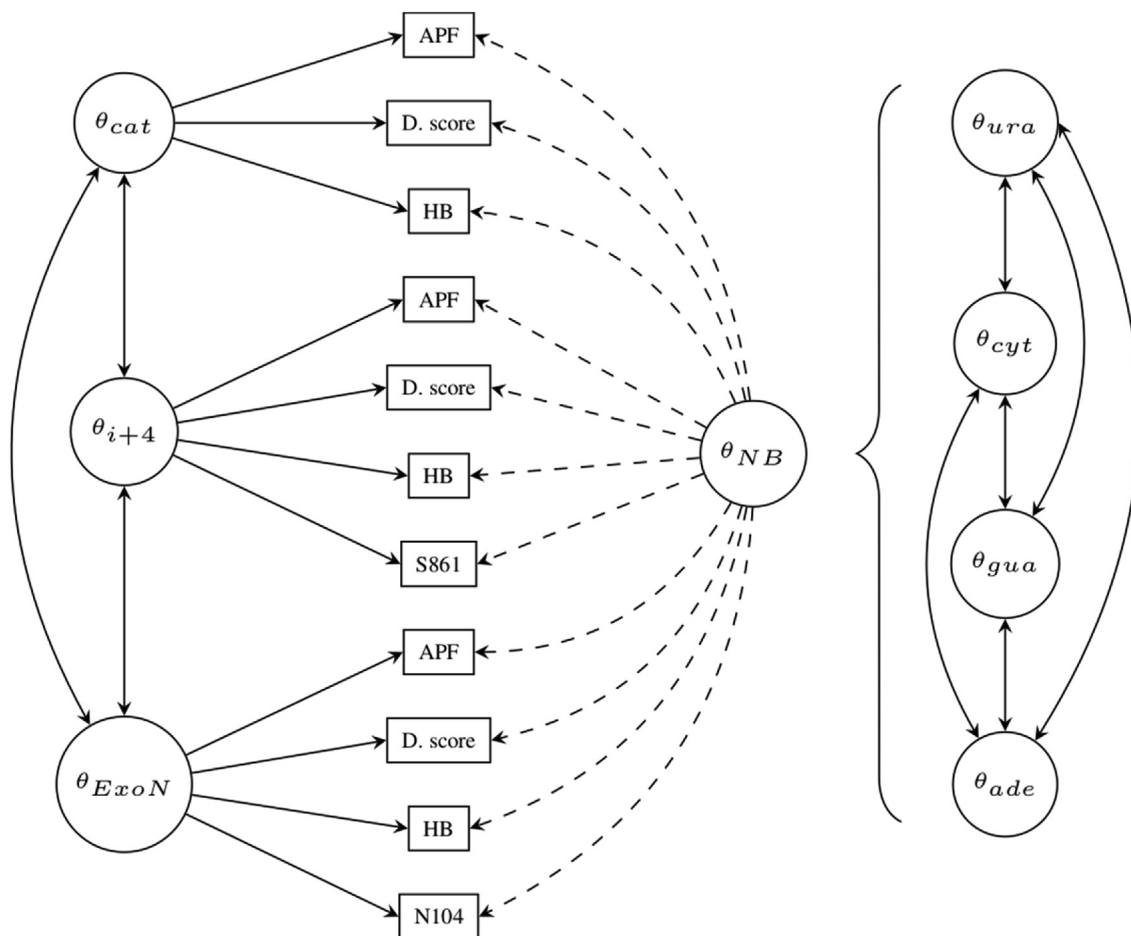


Fig. 5. Factorial design for the structural equations model used for estimating site consensus variables. This is a compact depiction presenting only 11 variables for one nitrogenous base system, but each of the four nitrogenous bases in the template RNA would have an identical structure (hence the dashed arrows). The rectangles represent observed variables, while circles are latent variables. Double-headed arrows represent admitted correlations; single-headed arrows represent factorial loadings. Cat: RdRp-cat; i + 4: RdRp-p4; ExoN: ExoN-cat; NB: nitrogenous base; ura: uracil; cyt: cytosine; gua: guanine; ade: adenine. D. score: docking score, APF: atomic property field, HB: hydrogen bonds score.

Funding

The authors thank the Mexico-Chile Fund 2020-Strategic Association Agreement 2006 (CH.02.UNAM, CH.06.UNAM) and the Institute of Chemistry, UNAM, for funding. JJN thanks CONACYT for a postdoctoral scholarship, and KM-M thanks DGAPA-PASPA for financial support. AB thanks the support of DGAPA-PAPIIT (IN214421). DGAPA-PAPIME (PE204921) is gratefully acknowledged by AL and RHM. The computations were supported by the Dirección General de Cómputo y de Tecnologías de Información y Comunicación (DGTIC)-UNAM, providing Miztli computer resources under grant LANCAD-UNAM-DGTIC-367.

Declaration of Competing Interest

The authors declare that they have no known competing financial interests or personal relationships that could have appeared to influence the work reported in this paper.

Acknowledgments

We gratefully acknowledge Jorge Peón-Peralta, Fernando Cortés Guzmán, Samuel Ponce de León-Rosales, Yolanda López-Vidal, René Arredondo, Patricia Orduña-Estrada for valuable discussions, proofread and comments on this manuscript.

Author contributions

K.M.M., A.M.M. and J.J.N. conceptualized and designed the project. A.M.M. and J.J.N. acquired the data, developed the methodology and analyzed the data. J.J.N., A.M.M., K.M.M., A.L., A.B., J.A.C.-B., R.H.M. and R.J. interpreted the results, wrote, and discussed the manuscript. The whole manuscript was approved by all authors.

Appendix A. Supplementary data

Supplementary data associated with this article can be found, in the online version, at <http://dx.doi.org/10.1016/j.csbj.2022.08.056>.

References

- [1] Adam D. The pandemic’s true death toll: millions more than official counts. Nature 2022;601:312–5. <https://doi.org/10.1038/d41586-022-00104-8>.
- [2] Thompson MG, Burgess JL, Naleway AL, Tyner H, Yoon SK, Meece J, et al. Prevention and attenuation of covid-19 with the BNT162b2 and mRNA-1273 vaccines. N Engl J Med 2021;385:320–9. https://doi.org/10.1056/NEJMOA2107058/SUPPL_FILE/NEJMOA2107058_DATA-SHARING.PDF.
- [3] Gorbalenya AE, Enjuanes L, Ziebuhr J, Snijder EJ. Nidovirales: evolving the largest RNA virus genome. Virus Res 2006;117:17–37. <https://doi.org/10.1016/J.VIRUSRES.2006.01.017>.
- [4] Cruz-González A, Muñoz-Velasco I, Cottom-Salas W, Becerra A, Campillo-Balderas JA, Hernández-Morales R, et al. Structural analysis of viral ExoN domains reveals polyphyletic hijacking events. PLoS ONE 2021;16:e0246981.

- [5] Dearlove B, Lewitus E, Bai H, Li Y, Reeves DB, Joyce MG, et al. A SARS-CoV-2 vaccine candidate would likely match all currently circulating variants. *Proc Natl Acad Sci U S A* 2020;117:23652–62. https://doi.org/10.1073/PNAS.2008281117/SUPPL_FILE/PNAS.2008281117.SAPP.PDF.
- [6] Ferron F, Subissi L, de Moraes ATS, Le NTT, Sevajol M, Gluais L, et al. Structural and molecular basis of mismatch correction and ribavirin excision from coronavirus RNA. *Proc Natl Acad Sci U S A* 2017;115:E162–71. https://doi.org/10.1073/PNAS.1718806115/SUPPL_FILE/PNAS.201718806SI.PDF.
- [7] Cohen J. Vaccines that can protect against many coronaviruses could prevent another pandemic. *Science* (1979) 2021. <https://doi.org/10.1126/science.abi9939>.
- [8] Rona G, Zeke A, Miwatani-Minter B, de Vries M, Kaur R, Schinlever A, et al. The NSP14/NSP10 RNA repair complex as a Pan-coronavirus therapeutic target. *Cell Death Different* 2021 29:2 2021;29:285–92. <https://doi.org/10.1038/s41418-021-00900-1>.
- [9] Murray CJL, Piot P. The potential future of the COVID-19 pandemic: will SARS-CoV-2 become a recurrent seasonal infection? *JAMA* 2021;325:1249–50. <https://doi.org/10.1001/JAMA.2021.2828>.
- [10] Coronaviridae. *Virus Taxonomy* 2012:806–28. <https://doi.org/10.1016/B978-0-12-384684-6.00068-9>.
- [11] Bukhari K, Mulley G, Gulyaeva AA, Zhao L, Shu G, Jiang J, et al. Description and initial characterization of metatranscriptomic nidovirus-like genomes from the proposed new family Abyssoviridae, and from a sister group to the Coronavirinae, the proposed genus Alphateovirus. *Virology* 2018;524:160–71. <https://doi.org/10.1016/J.VIROL.2018.08.010>.
- [12] Hartenian E, Nandakumar D, Lari A, Ly M, Tucker JM, Glaunsinger BA. The molecular virology of coronaviruses. *J Biol Chem* 2020;295:12910–34. <https://doi.org/10.1074/JBC.REV120.013930>.
- [13] Jácome R, Becerra A, de León SP, Lázcano A. Structural analysis of monomeric RNA-dependent polymerases: evolutionary and therapeutic implications. *PLoS ONE* 2015;10. <https://doi.org/10.1371/JOURNAL.PONE.0139001>.
- [14] Černý J, Černá Bolíková B, Paolo PM, Grubhoffer L, Růžek D. A deep phylogeny of viral and cellular right-hand polymerases. *Infect Genet Evol* 2015;36:275–86. <https://doi.org/10.1016/J.MEEGID.2015.09.026>.
- [15] Mõnttinen HAM, Ravantti JJ, Poranen MM. Structure unveils relationships between RNA virus polymerases. *Viruses* 2021;13. <https://doi.org/10.3390/V13020313>.
- [16] Mõnttinen HAM, Ravantti JJ, Stuart DI, Poranen MM. Automated structural comparisons clarify the phylogeny of the right-hand-shaped polymerases. *Mol Biol Evol* 2014;31:2741–52. <https://doi.org/10.1093/MOLBEV/MSU219>.
- [17] Kirchdoerfer RN, Ward AB. Structure of the SARS-CoV nsp12 polymerase bound to nsp7 and nsp8 co-factors. *Nat Commun* 2019 10:1 2019;10:1–9. <https://doi.org/10.1038/s41467-019-10280-3>.
- [18] Gao Y, Yan L, Huang Y, Liu F, Zhao Y, Cao L, et al. Structure of the RNA-dependent RNA polymerase from COVID-19 virus. *Science* 2020;368:779–82. <https://doi.org/10.1126/SCIENCE.ABB7498>.
- [19] Jácome R, Campillo-Balderas JA, Becerra A, Lázcano A. Structural analysis of monomeric RNA-dependent polymerases revisited. *J Mol Evol* 2022;90:283–95. <https://doi.org/10.1007/S00239-022-10059-Z>.
- [20] Lehmann KC, Gulyaeva A, Zevenhoven-Dobbe JC, Janssen GMC, Ruben M, Overkleeft HS, et al. Discovery of an essential nucleotidylating activity associated with a newly delineated conserved domain in the RNA polymerase-containing protein of all nidoviruses. *Nucleic Acids Res* 2015;43:8416–34. <https://doi.org/10.1093/NAR/GKV838>.
- [21] Ogando NS, Ferron F, Decroly E, Canard B, Posthuma CC, Snijder EJ. The curious case of the nidovirus exoribonuclease: its role in RNA synthesis and replication fidelity. *Front Microbiol* 2019;10:1813. <https://doi.org/10.3389/FMICB.2019.01813/BIBTEX>.
- [22] Smith EC, Blanc H, Vignuzzi M, Denison MR. Coronaviruses lacking exoribonuclease activity are susceptible to lethal mutagenesis: evidence for proofreading and potential therapeutics. *PLoS Pathog* 2013;9. <https://doi.org/10.1371/JOURNAL.PPAT.1003565>.
- [23] Agostini ML, Andres EL, Sims AC, Graham RL, Sheahan TP, Lu X, et al. Coronavirus susceptibility to the antiviral remdesivir (GS-5734) is mediated by the viral polymerase and the proofreading exoribonuclease. *MBio* 2018;9. <https://doi.org/10.1128/MBIO.00221-18/ASSET/A3FF74B2-3D2F-4D32-8CFF-6F258D2C4B92/ASSETS/GRAPHIC/MBO0011837620007.JPEG>.
- [24] Zhang L, Zhang D, Wang X, Yuan C, Li Y, Jia X, et al. 1'-Ribose cyano substitution allows Remdesivir to effectively inhibit nucleotide addition and proofreading during SARS-CoV-2 viral RNA replication. *PCCP* 2021;23:5852–63. <https://doi.org/10.1039/D0CP05948I>.
- [25] Naveja JJ, Madariaga-Mazón A, Flores-Murrieta F, Granados-Montiel J, Maradiaga-Ceceña M, Alaniz VD, et al. Union is strength: antiviral and anti-inflammatory drugs for COVID-19. *Drug Discov Today* 2021;26:229–39. <https://doi.org/10.1016/J.DRUIDIS.2020.10.018>.
- [26] Eslami G, Mousaviasl S, Radmanesh E, Jelvay S, Bitaraf S, Simmons B, et al. The impact of sofosbuvir/daclatasvir or ribavirin in patients with severe COVID-19. *J Antimicrob Chemother* 2020;75:3366–72. <https://doi.org/10.1093/JAC/DKAA331>.
- [27] Khater S, Kumar P, Dasgupta N, Das G, Ray S, Prakash A. Combining SARS-CoV-2 proofreading exonuclease and RNA-dependent RNA polymerase inhibitors as a strategy to combat COVID-19: a high-throughput in silico screening. *Front Microbiol* 2021;12. <https://doi.org/10.3389/FMICB.2021.647693>.
- [28] Robson F, Khan KS, Le TK, Paris C, Demirbag S, Barfuss P, et al. Coronavirus RNA proofreading: molecular basis and therapeutic targeting. *Mol Cell* 2020;79:710–27. <https://doi.org/10.1016/J.MOLCEL.2020.07.027>.
- [29] Hernández-Morales R, Becerra A, Campillo-Balderas JA, Cottom-Salas WF, Cruz-González A, Jácome R, et al. Structural biology of the SARS-CoV-2 replisome: evolutionary and therapeutic implications. *Biomedical Innov Comb* 2022:65–82. <https://doi.org/10.1016/B978-0-323-90248-9.00007-3>.
- [30] Avery ME. *Biographical Memoirs*, vol. 78. Washington, D.C.: National Academies Press; 2000. <https://doi.org/10.17226/9977>.
- [31] Khan S, Attar F, Bloukh SH, Sharif M, Nabi F, Bai Q, et al. A review on the interaction of nucleoside analogues with SARS-CoV-2 RNA dependent RNA polymerase. *Int J Biol Macromol* 2021;181:605–11. <https://doi.org/10.1016/J.IJBIOMAC.2021.03.112>.
- [32] Cai Q, Yang M, Liu D, Chen J, Shu D, Xia J, et al. Experimental treatment with favipiravir for COVID-19: an open-label control study. *Engineering (Beijing)* 2020;6:1192–8. <https://doi.org/10.1016/J.ENG.2020.03.007>.
- [33] Nourian A, Khalili H. Sofosbuvir as a potential option for the treatment of COVID-19. *Acta Bio Medica : Atenei Parmensis* 2020;91:239. <https://doi.org/10.23750/ABM.V9I12.9609>.
- [34] Tong S, Su Y, Yu Y, Wu C, Chen J, Wang S, et al. Ribavirin therapy for severe COVID-19: a retrospective cohort study. *Int J Antimicrob Agents* 2020;56. <https://doi.org/10.1016/J.IJANTIMICAG.2020.106114>.
- [35] Painter WP, Holman W, Bush JA, Almazedi F, Malik H, Eraut NCJE, et al. Human Safety, Tolerability, and Pharmacokinetics of Molnupiravir, a Novel Broad-Spectrum Oral Antiviral Agent with Activity Against SARS-CoV-2. *Antimicrob Agents Chemother* 2021;65. <https://doi.org/10.1128/AAC.02428-20>.
- [36] Yin YW, Steitz TA. The structural mechanism of translocation and helicase activity in T7 RNA polymerase. *Cell* 2004;116:393–404. [https://doi.org/10.1016/S0092-8674\(04\)00120-5/ATTACHMENT/854677DC-DF59-436A-9841-46321D3FB2EB/MMC2.AVI](https://doi.org/10.1016/S0092-8674(04)00120-5/ATTACHMENT/854677DC-DF59-436A-9841-46321D3FB2EB/MMC2.AVI).
- [37] Prussia AJ, Chennamadhavuni S. Biostructural Models for the Binding of Nucleoside Analogs to SARS-CoV-2 RNA-Dependent RNA Polymerase. *J Chem Inf Model* 2021;61:1402–11. https://doi.org/10.1021/ACS.JCIM.0C01277/SUPPL_FILE/C10C01277_SI_004.ZIP.
- [38] Bravo JPK, Dangerfield TL, Taylor DW, Johnson KA. Remdesivir is a delayed translocation inhibitor of SARS-CoV-2 replication. *Mol Cell* 2021;81:1548–1552.e4. <https://doi.org/10.1016/J.MOLCEL.2021.01.035>.
- [39] Gordon CJ, Tchesnokov EP, Woolner E, Perry JK, Feng JY, Porter DP, et al. Remdesivir is a direct-acting antiviral that inhibits RNA-dependent RNA polymerase from severe acute respiratory syndrome coronavirus 2 with high potency. *J Biol Chem* 2020;295:6785–97. <https://doi.org/10.1074/JBC.RA120.013679>.
- [40] Tchesnokov EP, Gordon CJ, Woolner E, Kocinkova D, Perry JK, Feng JY, et al. Template-dependent inhibition of coronavirus RNA-dependent RNA polymerase by remdesivir reveals a second mechanism of action. *J Biol Chem* 2020;295:16156–65. <https://doi.org/10.1074/JBC.ACI120.015720>.
- [41] Fischer W, Eron JJ, Holman W, Cohen MS, Fang L, Szewczyk LJ, et al. Molnupiravir, an Oral Antiviral Treatment for COVID-19. *MedRxiv* 2021. <https://doi.org/10.1101/2021.06.17.21258639>.
- [42] Ferron F, Sama B, Decroly E, Canard B. The enzymes for genome size increase and maintenance of large (+)RNA viruses. *Trends Biochem Sci* 2021;46. <https://doi.org/10.1016/J.TIBS.2021.05.006>.
- [43] Beigel JH, Tomashek KM, Dodd LE, Mehta AK, Zingman BS, Kalil AC, et al. Remdesivir for the treatment of covid-19 – final report. *N Engl J Med* 2020;383:1813–26. https://doi.org/10.1056/NEJM0A2007764/SUPPL_FILE/NEJM0A2007764_DATA-SHARING.PDF.
- [44] Bhimraj A, Morgan RL, Shumaker AH, Lavergne V, Baden L, Cheng VCC, et al. Infectious diseases society of america guidelines on the treatment and management of patients with COVID-19. *Clin Infect Dis* 2020. <https://doi.org/10.1093/CID/CIAA478>.
- [45] Nourian A, Khalili H, Ahmadinejad Z, Kouchak HE, Jafari S, Manshadi SAD, et al. Efficacy and safety of sofosbuvir/ledipasvir in treatment of patients with COVID-19: A randomized clinical trial. *Acta Bio Medica : Atenei Parmensis* 2020;91:1–14. <https://doi.org/10.23750/ABM.V9I14.10877>.
- [46] Hassanipour S, Arab-Zozani M, Amani B, Heidarzad F, Fathalipour M, Martinez-de-Hoyo R. The efficacy and safety of Favipiravir in treatment of COVID-19: a systematic review and meta-analysis of clinical trials. *Sci Rep* 2021;11. <https://doi.org/10.1038/s41598-021-90551-6>.
- [47] Elfiky AA. Anti-HCV, nucleotide inhibitors, repurposing against COVID-19. *Life Sci* 2020;248. <https://doi.org/10.1016/J.LFS.2020.117477>.
- [48] Pardo J, Shukla AM, Chamarthi G, Gupte A. The journey of remdesivir: from Ebola to COVID-19. *Drugs Context* 2020;9. <https://doi.org/10.7573/DIC.2020-4-14>.
- [49] Lawitz E, Mangia A, Wyles D, Rodriguez-Torres M, Hassanein T, Gordon SC, et al. Sofosbuvir for previously untreated chronic hepatitis C infection. *N Engl J Med* 2013;368:1878–87. <https://doi.org/10.1056/NEJM0A1214853>.
- [50] Gordon CJ, Tchesnokov EP, Schinazi RF, Götte M. Molnupiravir promotes SARS-CoV-2 mutagenesis via the RNA template. *J Biol Chem* 2021;297. <https://doi.org/10.1016/J.JBC.2021.100770/ATTACHMENT/7A610584-3A66-40B0-8D9D-5FFF69D149/MMCI.DOCX100770>.
- [51] Kocik G, Hillen HS, Tegunov D, Dienemann C, Seitz F, Schmitzova J, et al. Mechanism of SARS-CoV-2 polymerase stalling by remdesivir. *Nat Commun* 2021 12:1 2021;12:1–7. <https://doi.org/10.1038/s41467-020-20542-0>.
- [52] Malone B, Campbell EA. Molnupiravir: coding for catastrophe. *Nat Struct Mol Biol* 2021 28:9 2021;28:706–8. <https://doi.org/10.1038/s41594-021-00657-8>.
- [53] Kabinger F, Stiller C, Schmitzová J, Dienemann C, Kocik G, Hillen HS, et al. Mechanism of molnupiravir-induced SARS-CoV-2 mutagenesis. *Nat Struct Mol Biol* 2021 28:9 2021;28:740–6. <https://doi.org/10.1038/s41594-021-00651-0>.

- [54] Merck and Ridgeback's Investigational Oral Antiviral Molnupiravir Reduced the Risk of Hospitalization or Death by Approximately 50 Percent Compared to Placebo for Patients with Mild or Moderate COVID-19 in Positive Interim Analysis of Phase 3 Study - Merck.com n.d. <https://www.merck.com/news/merck-and-ridgebacks-investigational-oral-antiviral-molnupiravir-reduced-the-risk-of-hospitalization-or-death-by-approximately-50-percent-compared-to-placebo-for-patients-with-mild-or-moderate/> (accessed March 16, 2022).
- [55] Merck and Ridgeback Biotherapeutics Provide Update on Results from MOVE-OUT Study of Molnupiravir, an Investigational Oral Antiviral Medicine, in At Risk Adults With Mild-to-Moderate COVID-19 - Merck.com n.d. <https://www.merck.com/news/merck-and-ridgeback-biotherapeutics-provide-update-on-results-from-move-out-study-of-molnupiravir-an-investigational-oral-antiviral-medicine-in-at-risk-adults-with-mild-to-moderate-covid-19/> (accessed March 16, 2022).
- [56] Jácome R, Campillo-Balderas JA, Ponce de León S, Becerra A, Lazcano A. Sofosbuvir as a potential alternative to treat the SARS-CoV-2 epidemic. *Sci Rep* 2020;10:1–5. <https://doi.org/10.1038/s41598-020-66440-9>.
- [57] Eltahla AA, Luciani F, White PA, Lloyd AR, Bull RA. Inhibitors of the hepatitis C virus polymerase. *Mode Action Resistance Viruses* 2015;7:5206–24. <https://doi.org/10.3390/V7102868>.
- [58] Doharey PK, Singh V, Gedda MR, Sahoo AK, Varadwaj PK, Sharma B. In silico study indicates antimalarials as direct inhibitors of SARS-CoV-2-RNA dependent RNA polymerase. *J Biomol Struct Dyn* 2021. <https://doi.org/10.1080/07391102.2021.1871956>.
- [59] Jockusch S, Tao C, Li X, Anderson TK, Chien M, Kumar S, et al. A library of nucleotide analogues terminate RNA synthesis catalyzed by polymerases of coronaviruses that cause SARS and COVID-19. *Antiviral Res* 2020;180. <https://doi.org/10.1016/j.antiviral.2020.104857>.
- [60] Castanares-Zapatero D, Chalón P, Kohn L, Dauvrin M, Detollenaere J, Maertens de Noordhout C, et al. Pathophysiology and mechanism of long COVID: a comprehensive review. 2022;54:1473–87. <https://doi.org/10.1080/07853890.2022.2076901>.
- [61] Lopez-Leon S, Wegman-Ostrosky T, Perelman C, Sepulveda R, Rebolledo PA, Cuapio A, et al. More than 50 long-term effects of COVID-19: a systematic review and meta-analysis. *Scientific Reports* 2021;11:1–12. <https://doi.org/10.1038/s41598-021-95565-8>.
- [62] Buonsenso D, Piazza M, Boner AL, Bellanti JA. Long COVID: A proposed hypothesis-driven model of viral persistence for the pathophysiology of the syndrome. *Allergy Asthma Proc* 2022;43:187–93. <https://doi.org/10.2500/AAP.2022.43.220018>.
- [63] Phetsouphanh C, Darley DR, Wilson DB, Howe A, Munier CML, Patel SK, et al. Immunological dysfunction persists for 8 months following initial mild-to-moderate SARS-CoV-2 infection. *Nat Immunol* 2022;23:210–6. <https://doi.org/10.1038/s41590-021-01113-x>.
- [64] Tejerina F, Catalan P, Rodriguez-Grande C, Adan J, Rodriguez-Gonzalez C, Muñoz P, et al. Post-COVID-19 syndrome. SARS-CoV-2 RNA detection in plasma, stool, and urine in patients with persistent symptoms after COVID-19. *BMC Infect Dis* 2022;22:1–8. <https://doi.org/10.1186/s12879-022-07153-4/FIGURES/1>.
- [65] Zollner A, Koch R, Jukic A, Pfister A, Meyer M, Rössler A, et al. Postacute COVID-19 is characterized by gut viral antigen persistence in inflammatory bowel diseases. *Gastroenterology* 2022;163:495–506.e8. <https://doi.org/10.1053/j.gastro.2022.04.037>.
- [66] D'Abramo A, Vita S, Maffongelli G, Mariano A, Agrati C, Castilletti C, et al. Prolonged and severe SARS-CoV-2 infection in patients under B-cell-depleting drug successfully treated: A tailored approach. *Int J Inf Dis* 2021;107:247–50. <https://doi.org/10.1016/j.ijid.2021.04.068/ATTACHMENT/3C64F79B-FBD5-483E-9688-FE38C028C7F6/MMC1.DOCX>.
- [67] Dayco JS, El-Reda Z, Sumbal N, Alhusain R, Raheem S. Perpetually positive: post-COVID interstitial lung disease in an immunocompromised patient with diffuse large B-cell lymphoma. *J Invest Med High Impact Case Rep* 2021;9. <https://doi.org/10.1177/23247096211041207>.
- [68] Nussenblatt V, Roder AE, Das S, de Wit E, Youn JH, Banakis S, et al. Yearlong COVID-19 infection reveals within-host evolution of SARS-CoV-2 in a patient with B-Cell depletion. *J Infect Dis* 2022;225:1118–23. <https://doi.org/10.1093/infdis/jiab622>.
- [69] Kozlov M. Why scientists are racing to develop more COVID antivirals. *Nature* 2022;601:496. <https://doi.org/10.1038/D41586-022-00112-8>.
- [70] WHO Solidarity Trial Consortium. Repurposed antiviral drugs for covid-19 – interim WHO solidarity trial results. *N Engl J Med* 2021;384:497–511. https://doi.org/10.1056/NEJM0A2023184/SUPPL_FILE/NEJM0A2023184_DATA-SHARING.PDF.
- [71] Sidik SM. New COVID drugs face delays as trials grow more difficult. *Nature* 2022;606:637. <https://doi.org/10.1038/D41586-022-01602-5>.
- [72] Pitts J, Li J, Perry JK, du Pont V, Riola N, Rodriguez L, et al. Remdesivir and GS-441524 retain antiviral activity against delta, omicron, and other emergent SARS-CoV-2 variants. *Antimicrob Agents Chemother* 2022;66. <https://doi.org/10.1128/AAC.00222-22>.
- [73] Dagpunar J. Interim estimates of increased transmissibility, growth rate, and reproduction number of the Covid-19 B.1.617.2 variant of concern in the United Kingdom. *MedRxiv* 2021:2021.06.03.21258293. <https://doi.org/10.1101/2021.06.03.21258293>.
- [74] White JM, Schiffer JT, Bender Ignacio RA, Xu S, Kainov D, Ianevski A, et al. Drug Combinations as a First Line of Defense against Coronaviruses and Other Emerging Viruses. *MBio* 2021;12. <https://doi.org/10.1128/MBIO.03347-21>.
- [75] Abagyan R, Totrov M, Kuznetsov D. ICM—A new method for protein modeling and design: Applications to docking and structure prediction from the distorted native conformation. *J Comput Chem* 1994;15:488–506. <https://doi.org/10.1002/jcc.540150503>.
- [76] Schapira M, Totrov M, Abagyan R. Prediction of the binding energy for small molecules, peptides and proteins. *J Mol Recognit* 1999;12:177–90. [https://doi.org/10.1002/\(SICI\)1099-1352\(199905/06\)12:3<177::AID-IMR451>3.0.CO;2-Z](https://doi.org/10.1002/(SICI)1099-1352(199905/06)12:3<177::AID-IMR451>3.0.CO;2-Z).
- [77] Totrov M. Atomic property fields: Generalized 3D pharmacophoric potential for automated ligand superposition, pharmacophore elucidation and 3D QSAR. *Chem Biol Drug Des* 2008;71:15–27. <https://doi.org/10.1111/j.1747-0285.2007.00605.x>.
- [78] Biasini M, Bienert S, Waterhouse A, Arnold K, Studer G, Schmidt T, et al. SWISS-MODEL: modelling protein tertiary and quaternary structure using evolutionary information. *Nucleic Acids Res* 2014. <https://doi.org/10.1093/nar/gku340>.
- [79] Williams CJ, Headd JJ, Moriarty NW, Prisant MG, Videau LL, Deis LN, et al. MolProbity: more and better reference data for improved all-atom structure validation. *Protein Science: A Publication of the Protein Society* 2018;27:293. <https://doi.org/10.1002/PRO.3330>.
- [80] Rosseel Y. lavaan: an R package for structural equation modeling. *J Stat Softw* 2012;48:1–36. <https://doi.org/10.18637/jss.v048.i02>.